Synthesis & Characterization of Calcium Ruthenate (CRO) – Design of a Supercapacitor

S Pradhan[1], G S Roy[2*]

1. Kishore Nagar College, Cuttack, Odisha, India
2. Chairman CHSE, Bhubaneswar, Odisha, India
gsroy2004@gmail.com

Abstract: Calcium Ruthenate ($CaRuO_3$) has been synthesized by solution route method and characterized by analysis of TGA/DTA, XRD and SEM-EDX. Finally the V-I characteristic have been drawn from which the specific capacitance have been calculated the value indicate that this material ($CaRuO_3$) when used as an oxide electrode will act as a supercapacitor.

1.Introduction

Supercapacitors, also known as ultracapacitors or electrochemical double layer capacitors (EDLC), are electrochemical capacitors that have an unusually high energy density when compared to common capacitors, thousands times greater than a high-capacity electrolytic capacitor. For instance, a typical D-cell sized electrolytic capacitor will have a storage capacity measured in microfarad, while the same size supercapacitor would store several farads, an improvement of about 10,000 times. Larger commercial supercapacitors have capacities as high as 5,000 farads. Supercapacitors have a variety of commercial applications, notably in "energy smoothing" and momentary-load devices. Some of the earliest uses were motor startup capacitors for large engines in tanks and submarines, and as the cost has fallen they have started to appear on diesel trucks and railroad locomotives. More recently they have become a topic of some interest in the green energy world, where their ability to quickly soak up energy makes them particularly suitable for regenerative braking applications, whereas batteries have difficulty in this application due to slow charging time. They will make an excellent replacement for batteries in all-electric cars and plug-in hybrids, as they combine quick charging, temperature stability and excellent safety properties.
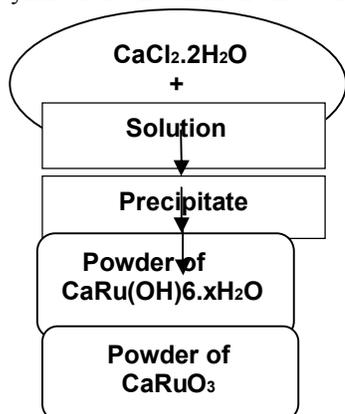
Due to the capacitor's high number of charge-discharge cycles (millions or more compared to 200–1000 for most commercially available rechargeable batteries) there were no disposable parts during the whole operating life of the device, which makes the device environment friendly. Batteries wear out on the order of a few years, and their highly reactive chemical electrolytes represent a serious disposal and safety hazard. This can be improved by only charging under favorable conditions, charging at an ideal rate and as rarely as possible. Supercapacitors can help in this regard, acting as a charge conditioner, storing energy from other sources for load balancing purposes and then using any excess energy to charge the batteries only at opportune times. As the energy density of supercapacitors is bridging the gap with batteries, it is hoped that in the near future the automotive industry will start to deploy ultracapacitors as a replacement for chemical batteries.The field of nanotechnology and nano-materials is exploding and is expected to develop into the next wave of technology rivaling microelectronics and biotech as well as contributing to both these sectors. Much of the interest in nano-materials is the result of the fact that material properties are markedly different than bulk materials. Nanosized ceramic particles are known for their ability to sinter at temperatures far below that of micron size particles. The purpose of this paper is to focus on some of the unique properties of nano-powders The important ideality of the ruthenates in this purpose is the ability to synthesize mono-disperse, smooth, high purity, non-agglomerated, dense, sub-micrometer sized powders with control over chemical homogeneity, crystallinity, crystalline phase content and microstructure. The conventional method to prepare metal ruthenates including bismuth ruthenate involves solid-state reactions of RuO_2 and respective metal oxides or their carbonates at high temperature under air or oxygen atmosphere with subsequent milling of the products to reduce the particle size [1–4]. These approaches do not allow good control over particle size, morphology, etc., in the micrometer to submicrometer region. Liquid phase routes have been used for preparation of ruthenate powders [5] and spray pyrolysis route has been used for preparation of sub-microcrystalline metal ruthenate powder [6]. But phase pure metal ruthenates have not formed by this route. Microstructure, crystalline and electrical properties of some TFRs are reported by Hrovat et al. [7], In this paper, we present the solution

route synthesis of calcium ruthenate ($CaRuO_3$) by co-precipitation of $CaCl_2.12H_2O$ and $RuCl_3xH_2O$ at pH 9.41 and dried at 100 ^{o}C in air at 250 ^{o}C in vacuum and their characterization by TGA/DTA, XRD, SEM-EDX.

2. Solution route synthesis of calcium ruthenate (CRO)

The experiment includes Stoichiometric amount of $CaCl_2.12H_2O$ and $RuCl_3.xH_2O$ are dissolved separately in 0.04% (w/w; 1.0 mM) CetylTrimethyl ammonium bromide (CTAB) solution as surfactant. The two solutions were mixed, stirred and the pH of the mixture was slowly increased up to 9.41 by addition of dilute NaOH. The reaction mixture was maintained at pH between 9.41 by using dilute HCl and NaOH solutions for about 1 h by constant stirring. The reaction mixture was allowed to settle for an hour, filtered and washed with distilled water and the powder was dried at 100 ^{o}C. The dried sample was ground to fine powder. This powder was further dried in vacuum oven at 250 ^{o}C for 4 h. The synthesis is shown in the flow chart 1.

```
      ┌─────────────────────┐
      │   CaCl₂.2H₂O        │
      │        +            │
      ├─────────────────────┤
      │     Solution        │
      └─────────────────────┘
                │
      ┌─────────────────────┐
      │    Precipitate      │
      └─────────────────────┘
                │
      ┌─────────────────────┐
      │    Powder of        │
      │   CaRu(OH)6.xH₂O    │
      └─────────────────────┘
                │
      ┌─────────────────────┐
      │    Powder of        │
      │     CaRuO₃          │
      └─────────────────────┘
```

Flow Chart-1

3. Characterization

The solution synthesized nano-powders of calcium ruthenate were characterized by the following instruments. Thermal stability of ruthenate powder was investigated by using thermal analyser (Mettler, Toledo, Model 851e) in dynamic nitrogen atmosphere in the temperature range 25 ^{o}C to 800 ^{o}C. Surface morphology, particle size and elemental composition were determined by using Scanning Electron Microscope-Energy Dispersive X-ray Analyser(SEM-EDX, Model XL 30, Philips, Holland). X-ray diffractograms (XRD) were recorded on X-ray diffractometer (X-ray Generator, Model PW 1729, Philips, Holland) by using CuKa (k =1.5405 A ^{o}) and Ni as the filter.

3.1 Electrode Preparation

Electrodes were prepared by painting slurry of the powder mixed with a solution of water and Triton X-100 (10:1) on nickel foils. These foils were previously etched in boiling HCl to remove oxide layers and to roughen the surface. The foils were point welded to a nickel wire as a current lead. To attach the coating and to burn out the binder the electrodes were annealed at 300–400°C for 2h in air after painting. The electrodes were 15×15 mm^2 and coated on one side only. Typical amounts of active mass were in the range of 2 mg cm^{-2}, which was determined by difference weighing before and after the coating. There was no detectable weight change of uncoated nickel foils due to surface oxidation of the nickel foil after such an annealing procedure.

3.2 Thermal analysis

Thermograms (TGA/DTA) of pristine powder of solution route as synthesized calcium ruthenate precipitated at pH 9.41 and dried at 100 ^{o}C are reproduced in Fig. 2.
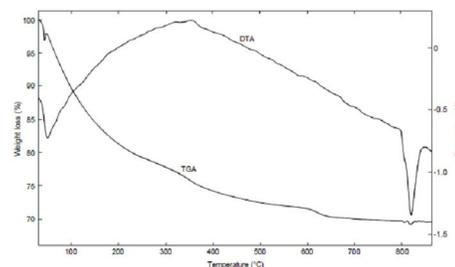

Fig. 1. TGA/DTA of n-$CaRuO_3$.

The first weight loss is due to water elimination up to 210 ^{o}C and the second weight loss is due to the formation of Ca and Ru complex hydroxides. The third weight loss is due the formation of $CaRuO_3$ up to 620 ^{o}C and there is a endothermic peak at 820 ^{o}C in DTA which shows that a fraction (δ) of oxygen is lost at 820 ^{o}C.

3.3. XRD analysis

Fig. 2 is the XRD of calcium ruthenate (CRO) prepared at pH 9.41 by solution route and dried at 250 ^{o}C in air. The theoretical and experimental values of $CaRuO_3$ are tabulated in Table 1. The majority of the peaks matches with the reported calcium ruthenate [8].
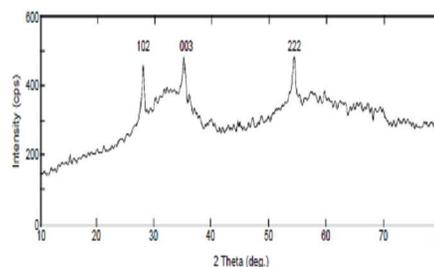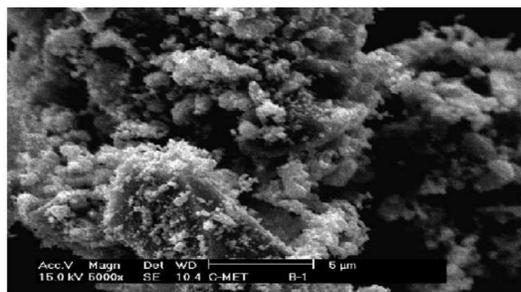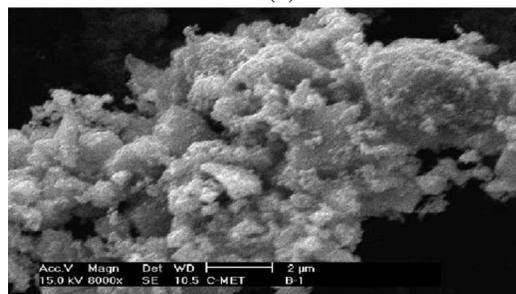

Figure2: XRD of n-$CaRuO_3$.

The three XRD major peaks of $CaRuO_3$ which are matching with the RuO_2 peaks [9], which is tolerant to electrical studies of fired TFRs of $CaRuO_3$. Because the nature of the particles is in the nano level, the peaks are broadened with less crystallinity.

3.4. Scanning electron microscopic (SEM)-EDX analyses

Fig. 4 shows the scanning electron micrographs of calcium ruthenate. The fine particles of $CaRuO_3$ prepared in the presence of CTAB at around its critical micellar concentration (CMC; 0.96 mM) of 1.0 mM were found to be in the nanometer range. We couldn't calculate the exact particle size of our sample of $CaRuO_3$ by SEM studies so that it is calculated by Scherrer's formula using XRD data of 12 nm instead. If the $CaRuO_3$ powder prepared by co-precipitation route without CTAB, the particle size will be around 150–250 nm which was observed by us in the case of $Bi_2Ru_2O_7$. We also achieved the particle size of $CaRuO_3$ by solid-state route using $CaCO_3$ and RuO_2 around 300–400 nm [10]. Fig. 5 is the representative EDAX spectrum of the calcium ruthenate powder. From this analysis, we confirmed the presence of Ca, Ru and O and estimated their relative atomic percentages.
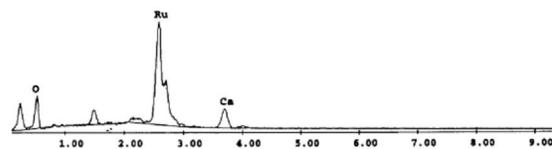

(a)

(b)

Fig. 3. SEM micrographs of a) nanosized CRO (×4000), b) nanosized CRO (×8000).

EDAX ZAF Quantification (Standardless)
Element Normalized

Element	Wt %	At %	K-Ratio	Z	A	F
O K	26.27	65.39	0.0478	1.1754	0.1548	1.0001
RuL	64.46	25.40	0.5904	0.8903	1.0263	1.0024
CaK	9.27	9.21	0.0820	1.0927	0.8092	1.0000
Total	100.00	100.00				

Fig. 4. EDX of n-$CaRuO_3$.

3.5 Characteristic I-V Curve

A three electrode arrangement in a beaker type class cell was used to determine the electrochemical behavior. The counter electrode consisted of a platinum sheet. Hg/HgO was used as the reference electrode in the same electrolyte. The electrolyte was 6M KOH. Cyclic voltammograms at various voltage sweep rates were recorded using an EG&G PAR model 273 potentiostat, controlled by a microcomputer. Specific capacitances were calculated by integrating the current of a CV half cycle and relating the charge to the voltage range and the weight of the active mass. Because the mass utilization of the porous active layer is very good the current densities in the CV diagrams are given with respect to the active mass loading rather than to the geometric area. CV diagrams of different materials can be compared more easily and do not depend on electrode loading.
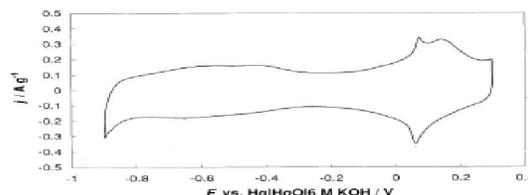

Fig 5 : CV taken at 20 mV s^{-1} of co precipitated $CaRuO_3$

4. Conclusion

In conclusion, it is summarized that Strontium Ruthenate nanomaterial is successfully synthesized in room temperature and pressure. In TGA/DTA, we have shown that the first weight loss is due to water elimination up to 120 ^{o}C and the second weight loss is due to the formation of Ca and Ru complex hydroxides. The third   weight loss is due the formation of $CaRuO_3$ up to 420°C and there is a endothermic peak at 720°C in DTA which shows that a fraction (δ) of oxygen is lost at 820°C. This SEM image clearly shows the morphology of $CaRuO_3$ nanoparticles with an average particle size of 50-100 nm. The majority of the peaks matches with the

reported strontium ruthenate. The three XRD major peaks of $CaRuO_3$ which are matching with the RuO_2 peaks. From the Characteristic I-V curve specific capacitances were calculated and the values indicates that this material when used as an oxide electrode capacitance will be act as supercapacitor.

References
[1] R.J. Bouchard, J.L. Gillson, Mater. Res. Bull. 6 (1971) 669.
[2] W. Bensch, H.W. Schmalle, A. Reller, Solid State Ionics 43 (1990)171.
[3] T. Yamamoto, R. Kanno, Y. Takeda, O. Yamamoto, Y. Kawamoto, M.Takano, J. Solid State Chem. 109 (1994) 372.
[4] A.T. Ashcroft, A.K. Cheetham, M.L.H. Green, C.P. Grey, P.D.F.Vernon, J. Chem. Soc., Chem. Commun. (1989) 1667.
[5] P.F. Carcia, A. Ferretti, A. Suna, J. Appl. Phys. 53 (1982) 5282.
[6] Y. Senzaki, M.J. Hampden-Smith, T.T. Kodas, J.W. Hussler, J. Am.Ceram. Soc. 78 (1995) 2977.
[7] M. Hrovat, Z. Samardzija, J. Holz, D. Belavic, J. Mater. Sci., Mater.Electron. 11 (2000) 1991.
[8] ASTM card No. 25– 172.
[9] ASTM card No. 21– 1172.
[10] K. Gurunathan, N.P. Vyawahare, D.P. Amalnerkar, J. Mater. Sci.,Mater. Electron. 16 (2005) 47– 53.

1/8/2013